Impacts of Sulfate Reduction on Phosphorus Cycling: Stability of Vivianite in Lake Sediments

Von der Fakultät für Umwelt und Naturwissenschaften
der Brandenburgischen Technischen Universität Cottbus-Senftenberg
zur Erlangung des akademischen Grades eines
Doktors der Naturwissenschaften (Dr. rer. nat.)

genehmigte Dissertation

vorgelegt von

M.Sc. in Earth Sciences

Harm Noël van Kuppevelt

aus Zeist, Königreich der Niederlande

Gutachter: M Hupfer
Tag der mündlichen Prüfung: May 2025

Planet Earth is blue
and there's nothing we can do
David Bowie

Contents

Summary

This is the document

Second paragraph of abstract starts here.

Zusammenfassung

This is the abstract in German

Second paragraph of abstract starts here.

Chapter 1

Introduction

Per Morgen- SEM-EDS SDU lab technicians Aarhus people

1.1 The Phosphorus problem

The emergence of humans on earth was followed by unprecedented changes in the Earths environment and disruption of the vital biogeochemical cycles underpinning the regenerative nature that characterized the climatologically stable Holocene epoch. As a species that can recognize the importance of live and its essential building blocks, we bear the responsibility of a fair and sustainable distribution of the earths resources. Unfortunately, externalizing impacts in favor of short-term profit has become humanities predominant mode of operation. The limits of regeneration are increasingly crossed, as described by the planetary boundary framework ((Richardson et al., 2023)). One of the transgressed boundaries is that of Phosphorus (P). The geological P cycle, P weathering from rocks flow in the ocean where it precipitates again, is a slow process, and many ecosystems are P limited. As an essential building block of life, P is recycled efficiently in natural ecosystems. Since the green revolution, agriculture is increasingly dependent on the use of fertilizer derived from phosphate rock (Ashley et al., 2011). This has broken the P cycle, instead forming a linear process with major implications at both ends of the chain (Cordell, 2010). On one end, food production has become dependent on a finite reservoir of phosphate rock, while accumulation of P in freshwater ecosystems causes wide spread ecological damage at the other end (Fig. 1.1). Harmful algae blooms through eutrophication threaten water quality and many related ecosystem services (Ansari and Gill, 2014). Closing the P cycle requires not just the reuse of P in agriculture, but also the restoration of lake ecosystems.

1.2 Phosphorus cycling in freshwater sediments

Talk about all the different forms P enters the sediment, and the early diagenesis.

The retention of P in sediments occurs through its binding to the solid phase via biological and chemical precipitation (Boers et al., 1998; O'Connell et al., 2020; Parsons et al., 2017). Burial P pools accumulate in sediment following years of nutrient enrichment. The speciation of sediment P is highly dependent on lake conditions and undergoes significant changes during

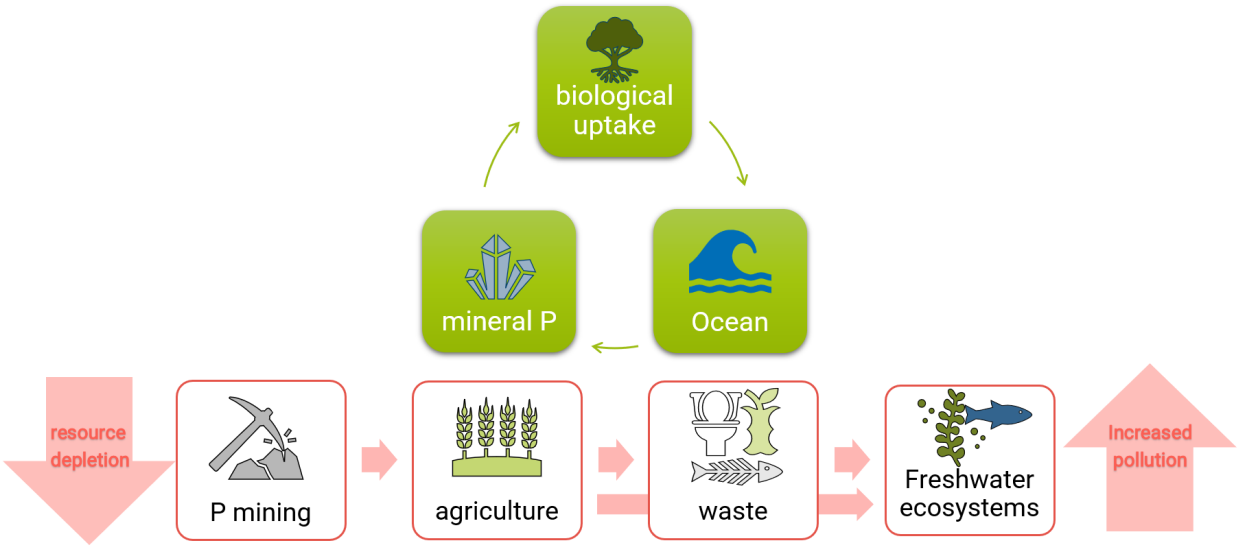

Figure 1.1: Top: geological P cycle. Bottom: Unstustainable P use. A finite resource of phosphate rock is used in agriculture and ends up in aquatic ecosystems, where it causes ecological damage.

early diagenesis, where remobilisation of labile forms of P occurs, whereas only the stable forms of solid-bound P are buried long-term (Boers et al., 1998; Emerson, 1976). Initially, the sedimentation of P incorporated into organic matter (OM) by primary producers is an important influx of P to lake sediments, especially in eutrophic lakes. However, the long-term burial of OM-bound P is constrained by remineralisation processes in the sediment (Boers et al., 1998). Secondly, P can adsorb to iron (Fe) hydroxides (Gunnars et al., 2002) and bind to OM to form organic Fe-P complexes (Fe(III)-OM-P) (Schwertmann and Murad, 1988). The precipitation of these ferric iron-bound P forms (Fe(III)-P) can be a major internal sink of P in lakes with naturally high Fe content (Hupfer and Lewandowski, 2008; Reitzel et al., 2005) or those artificially treated with Fe (Kleeberg et al., 2012; Münch et al., 2024). Under the reducing conditions induced by organic matter decomposition in the sediment, Fe(III) is reduced to Fe(II), leading to the release of bound P and preventing the long-term burial of Fe(III)-bound P. However, P can be sequestered long-term in the form of the Fe(II) mineral vivianite (Fe(II)3(PO4)2 · 8H2O) (Rothe et al., 2016), which has been identified as a major form of burial P in eutrophic, high-Fe, and nonsulphidic freshwater systems (Dijkstra et al., 2018; Kubeneck et al., 2021; O'Connell et al., 2015; Rothe, 2016).

1.3 Sulfur biogeochemistry

Basically summarize Zak et al. (2021).

– This analysis revealed three main clusters of research: one focused on biogeochemical processes in wetlands and lakes (emphasizing carbon, nitrogen, and methane dynamics), another on the ecotoxicological effects of sulfate (with emphasis on eutrophication and toxicity

in various species), and a third on bioremediation approaches to mitigate sulfate pollution.

3. Impact on Biogeochemical Cycles • Carbon Cycle: – Elevated sulfate levels can alter primary production, organic matter decomposition, and the overall balance between methane (CH) and carbon dioxide (CO) production. – Under anaerobic conditions, sulfate-reducing bacteria (SRB) become energetically favored over methanogens, shifting the electron flow from methanogenesis (which produces CH) to sulfate reduction (producing CO). – This transition can result in a diversion of carbon flow, potentially enhancing overall carbon mineralization rates and influencing greenhouse gas emissions.

• Phosphorus Cycle: – Sulfate reduction in sediments can lead to the production of sulfide, which in turn affects iron chemistry. – The reduction of Fe(III) compounds and subsequent precipitation of iron sulfides can liberate phosphate from sediments, thereby increasing its availability in the water column—a process sometimes referred to as "internal eutrophication." – This mechanism is especially critical in systems with high iron-bound phosphorus, where changes in the Fe:PO ^{3} ratio can trigger a net release of phosphorus into the water.

4. Ecotoxicological Effects and Human Health Implications • Toxicity to Aquatic Organisms: – Although sulfate itself is often considered one of the less toxic major ions, its presence can induce osmotic stress. The paper details that many freshwater species (e.g., invertebrates, certain fish, amphibians, and aquatic plants) exhibit reduced physiological performance at elevated sulfate concentrations. – Sensitivity to sulfate often depends on water chemistry; for instance, higher water hardness and the presence of chloride can mitigate some toxic effects, whereas soft water systems are more vulnerable.

• Role of Sulfide: – The ecotoxicological concern is compounded by the fact that sulfate reduction yields hydrogen sulfide (H S), a compound known for its high toxicity to aquatic life. – Elevated levels of sulfide can affect respiration, growth, and reproduction across a range of organisms, thereby impacting community structure and ecosystem services.

• Human Health Considerations: – The review also touches on potential implications for human health, particularly in relation to drinking water quality. – Many freshwater sources used for human consumption can be affected by sulfate levels, which in turn are regulated by environmental quality standards that consider both sulfate and its metabolites.

5. Bioremediation Strategies • Mitigation Approaches: – The paper reviews a variety of bioremediation techniques aimed at reducing sulfate loads in contaminated water bodies. – Constructed wetlands, permeable reactive barriers, and bioreactors are evaluated, with reported removal efficiencies ranging from 0% to 70%. – While promising, these technologies are highly variable in performance due to factors such as hydraulic residence time, microbial community composition, and the specific chemical environment.

• Research Gaps and Future Directions: – The authors emphasize that there is a pressing need for more field-scale studies to better understand the long-term trends and spatial dynamics of sulfate pollution. – They call for further research into the interactions between sulfate pollution, climate change, and land-use practices, as well as the development of more robust and scalable bioremediation systems.

6. Conclusions • The review concludes that the global perturbation of the sulfur cycle—driven by both legacy pollution and ongoing anthropogenic activities—is likely to have widespread and long-lasting effects on freshwater ecosystems. • The interplay between sulfate and major biogeochemical cycles is complex, influencing greenhouse gas emissions, nutrient dynamics, and ecological health. • There is a critical need for integrative, interdisciplinary research to refine our understanding of these processes and to develop effective mitigation strategies that protect both ecosystem function and human health.

This detailed synthesis provides a thorough overview suitable for researchers interested in the environmental chemistry, ecological impacts, and remediation of sulfate pollution in freshwater systems. For further details, please refer to the full article by Zak et al. (2020) in Earth-Science Reviews.

1.3.1 Sources and sinks for sulfur

Sources and Trends of Sulfate in Freshwaters • Natural versus Anthropogenic Inputs: – The review begins by distinguishing between natural sulfate sources—such as mineral weathering, volcanic emissions, sea spray aerosols, and the oxidation of naturally occurring sulphides—and anthropogenic sources. – Anthropogenic activities such as industrial emissions, acid mine drainage (AMD), wetland drainage, agricultural fertilization, and even historical practices (e.g., fertilization with sulfate-containing superphosphate) have substantially increased sulfate loads in many regions. – Despite significant reductions in atmospheric sulfur deposition in parts of North America and Europe (owing to improved emission controls), many freshwater bodies still show sulfate concentrations well above natural background levels. Sulphides are formed by both desulphuration and dissimilatory sulphate reduction leading to a higher degree of sediment sulphidization. The former can be quite significant in overall sedimentary hydrogen sulphide production, e.g. 5.1 - 53 % (Dunnette et al., 1985).

1.3.2 Interactions between sulfur cycling and eutrophication.

(Due to eutrophication, i.e. a primarily enhanced P supply, the P-binding capacity of a sediment will be exceeded leading to a higher P mobility and less or no vivianite formation. A higher productivity leads to a higher OM supply toward the sediment which has consequences for the formation of vivianite. First, there is a higher demand for oxidants leading to a deterioration of redox conditions and higher reduction rates of ferric Fe and SO24 (Holmer & Storkholm, 2001). Second, there is more S2– produced because OM is specifically enriched in S compared to Fe (Redfield ratio: C106N16P1S0.7Fe0.05, [Stumm1981]). Moreover, eutrophication is often accompanied by considerable inputs of SO24 leading to

its higher availability and high rates of its consumption (Holmer and Storkholm, 2001; Zak et al., 2006). Third, the OM itself can react with Fe forming a metal organic complex (Lalonde et al., 2012). The higher the sedimentary S:Fe ratio, the less reactive Fe seems to be available reducing the potential of vivianite to form (Fig. 3.5) because more Fe is bound in sulphidic form. Thus, under eutrophic conditions there is a negative feedback evolving through the enhanced supply of OM lowering the sedimentary P retention capacity due to less vivianite. Aquatic systems naturally high in reactive Fe may compensate better for a eutrophication induced decrease in P retention than systems low in Fe. This implies, that an artificial supply of Fe to systems with a high level in OM, P and SO24 can be used as a successful measure of lake restoration leading to increased P retention through vivianite formation (Kleeberg et al. (2013); Rothe et al. (2014)). To ensure a lasting effect on P burial, Fe has to be supplied in surplus compensating for the losses through FeSx formation (Kleeberg et al., 2013) and the reaction with OM (Lalonde et al. (2012)). At which magnitude vivianite finally forms in different types of sediments depends on multiple factors and remains to be further investigated. The formation of the mineral is also controlled by the availability of OM rich in P, the concomittant liberation of Fe2+ and PO34 into the pore voids of the sediment, the activity of microorganisms and resorption of PO34 onto the surface of remaining iron(oxyhydr)oxides.) Rothe 2015

1.4 Vivianite in the sediment

Start at the beginning, vivianite characteristics. basically summarize Rothe (2016) Next, the formation requirments and kinetics (Paskin, 2024) Then, the stability under oxygen conditions And then the part about the sulfidation

$$Fe_3(PO_4)_2 \bullet H_2O(s) + 2H^+ \rightleftharpoons 3Fe^{2+} + 2HPO_4^{2-} + 8H_2O \tag{1.1}$$

$$Fe^{2+} + xHS^- \rightleftharpoons FeS_x(s) + xH^+ \tag{1.2}$$

1.5 Research objectives and outline

The research presented in this dissertation was done as part of the EU Horizon 2020 Marie Curie Innovative training network “RecaP”. The goal of the RecaP project is to better understand the impact and changes needed to reach a sustainable use of P. The research here focuses on the cycling of P in freshwater systems, which needs to be understood in order to improve water quality. Specifically, the sulfide-induced mobilization of P from vivianite is investigated in lake sediments. The background and state of the knowledge is outlined in chapter 1. Although it has been shown that vivianite reacts with sulfide under laboratory conditions, the process has not been studied directly in natural lake sediment. The dissertation aims to answer the following research questions:

- Can sulfide produced by microbial sulfate reduction mobilize P from vivianite in lake sediment?

- What is the potential relevance of vivianite destabilization for sediment P retention capacity?

The process is studied in different contexts relevant for restoration of eutrophic lakes: In chapter 2, the stability of vivianite and other Fe-bound P forms is assessed after treating the sediment with Fe, to demonstrate the limits of Fe amendment as restoration technique. Chapter 3 addresses the relevance of legacy P bound in vivianite as possible source of P, and in chapter 4 this is further investigated under natural conditions. Chapter 5 summarizes the outcomes of the other chapters and places the findings in a broader context.

Chapter 2

Investigating the persistance of iron-bound phosphorus in lake sediments under sulfidic conditions

Here is a brief introduction into using *R Markdown*. *Markdown* is a simple formatting syntax for authoring HTML, PDF, and MS Word documents. *R Markdown* provides the flexibility of *Markdown* with the implementation of **R** input and output. For more details on using *R Markdown* see `https://rmarkdown.rstudio.com`.

Be careful with your spacing in *Markdown* documents. While whitespace largely is ignored, it does at times give *Markdown* signals as to how to proceed. As a habit, try to keep everything left aligned whenever possible, especially as you type a new paragraph. In other words, there is no need to indent basic text in the Rmd document (in fact, it might cause your text to do funny things if you do).

2.1 Lists

It's easy to create a list. It can be unordered like

- Item 1
- Item 2

or it can be ordered like

1. Item 1
2. Item 2

Notice that I intentionally mislabeled Item 2 as number 4. *Markdown* automatically figures this out! You can put any numbers in the list and it will create the list. Check it out below.

To create a sublist, just indent the values a bit (at least four spaces or a tab). (Here's one case where indentation is key!)

1. Item 1

2. Item 2
3. Item 3
    - Item 3a
    - Item 3b

2.2 Line breaks

Make sure to add white space between lines if you'd like to start a new paragraph. Look at what happens below in the outputted document if you don't:

Here is the first sentence. Here is another sentence. Here is the last sentence to end the paragraph. This should be a new paragraph.

Now for the correct way:

Here is the first sentence. Here is another sentence. Here is the last sentence to end the paragraph.

This should be a new paragraph.

2.3 R chunks

When you click the **Knit** button above a document will be generated that includes both content as well as the output of any embedded **R** code chunks within the document. You can embed an **R** code chunk like this (`cars` is a built-in **R** dataset):

2.4 Inline code

If you'd like to put the results of your analysis directly into your discussion, add inline code like this:

> The `cos` of 2π is 1.

Another example would be the direct calculation of the standard deviation:

> The standard deviation of `speed` in `cars` is 5.2876444.

One last neat feature is the use of the `ifelse` conditional statement which can be used to output text depending on the result of an **R** calculation:

> The standard deviation is less than 6.

Note the use of `>` here, which signifies a quotation environment that will be indented.

As you see with `$2 \pi$` above, mathematics can be added by surrounding the mathematical text with dollar signs. More examples of this are in Mathematics and Science if you uncomment the code in Math.

2.5 Including plots

You can also embed plots. For example, here is a way to use the base **R** graphics package to produce a plot using the built-in `pressure` dataset:

Note that the `echo=FALSE` parameter was added to the code chunk to prevent printing of the **R** code that generated the plot. There are plenty of other ways to add chunk options (like `fig.height` and `fig.width` in the chunk above). More information is available at `https://yihui.org/knitr/options/`.

Another useful chunk option is the setting of `cache=TRUE` as you see here. If document rendering becomes time consuming due to long computations or plots that are expensive to generate you can use knitr caching to improve performance. Later in this file, you'll see a way to reference plots created in **R** or external figures.

2.6 Loading and exploring data

Included in this template is a file called `flights.csv`. This file includes a subset of the larger dataset of information about all flights that departed from Seattle and Portland in 2014. More information about this dataset and its **R** package is available at `https://github.com/ismayc/pnwflights14`. This subset includes only Portland flights and only rows that were complete with no missing values. Merges were also done with the `airports` and `airlines` data sets in the `pnwflights14` package to get more descriptive airport and airline names.

We can load in this data set using the following commands:

```
# flights.csv is in the data directory
flights_path <- here::here("data", "flights.csv")
# string columns will be read in as strings and not factors now
flights <- read.csv(flights_path, stringsAsFactors = FALSE)
```

The data is now stored in the data frame called `flights` in **R**. To get a better feel for the variables included in this dataset we can use a variety of functions. Here we can see the dimensions (rows by columns) and also the names of the columns.

```
dim(flights)
```

```
## [1] 12649    16
```

```
names(flights)
```

```
##  [1] "month"        "day"          "dep_time"     "dep_delay"
##  [5] "arr_time"     "arr_delay"    "carrier"      "tailnum"
##  [9] "flight"       "dest"         "air_time"     "distance"
## [13] "hour"         "minute"       "carrier_name" "dest_name"
```

Another good idea is to take a look at the dataset in table form. With this dataset having more than 20,000 rows, we won't explicitly show the results of the command here. I recommend you enter the command into the Console ***after*** you have run the **R** chunks above to load the data into **R**.

```
View(flights)
```

While not required, it is highly recommended you use the `dplyr` package to manipulate and summarize your data set as needed. It uses a syntax that is easy to understand using chaining operations. Below I've created a few examples of using `dplyr` to get information about the Portland flights in 2014. You will also see the use of the `ggplot2` package, which produces beautiful, high-quality academic visuals.

We begin by checking to ensure that needed packages are installed and then we load them into our current working environment:

```
# List of packages required for this analysis
pkg <- c("dplyr", "ggplot2", "knitr", "bookdown")
# Check if packages are not installed and assign the
# names of the packages not installed to the variable new.pkg
new.pkg <- pkg[!(pkg %in% installed.packages())]
# If there are any packages in the list that aren't installed,
# install them
if (length(new.pkg)) {
  install.packages(new.pkg, repos = "https://cran.rstudio.com")
}
# Load packages
library(thesisdown)
library(dplyr)
library(ggplot2)
library(knitr)
```

The example we show here does the following:

- Selects only the `carrier_name` and `arr_delay` from the `flights` dataset and then assigns this subset to a new variable called `flights2`.
- Using `flights2`, we determine the largest arrival delay for each of the carriers.

```
flights2 <- flights %>%
  select(carrier_name, arr_delay)
max_delays <- flights2 %>%
  group_by(carrier_name) %>%
  summarize(max_arr_delay = max(arr_delay, na.rm = TRUE))
```

A useful function in the `knitr` package for making nice tables in *R Markdown* is called `kable`. It is much easier to use than manually entering values into a table by copying and pasting values into Excel or LaTeX. This again goes to show how nice reproducible documents can be! (Note the use of `results="asis"`, which will produce the table instead of the code to create the table.) The `caption.short` argument is used to include a shorter title to appear in the List of Tables.

```
kable(max_delays,
  col.names = c("Airline", "Max Arrival Delay"),
  caption = "Maximum Delays by Airline",
  caption.short = "Max Delays by Airline",
  longtable = TRUE,
  booktabs = TRUE
)
```

Table 2.1: Maximum Delays by Airline

Airline	Max Arrival Delay
Alaska Airlines Inc.	338
American Airlines Inc.	1539
Delta Air Lines Inc.	371
Frontier Airlines Inc.	166
Hawaiian Airlines Inc.	116
JetBlue Airways	256
SkyWest Airlines Inc.	321
Southwest Airlines Co.	315
US Airways Inc.	347
United Air Lines Inc.	319
Virgin America	366

The last two options make the table a little easier-to-read.

We can further look into the properties of the largest value here for American Airlines Inc. To do so, we can isolate the row corresponding to the arrival delay of 1539 minutes for American in our original `flights` dataset.

```
flights %>%
  filter(
    arr_delay == 1539,
    carrier_name == "American Airlines Inc."
  ) %>%
  select(-c(
    month, day, carrier, dest_name, hour,
    minute, carrier_name, arr_delay
  ))
```

```
##   dep_time dep_delay arr_time tailnum flight dest air_time distance
## 1     1403      1553     1934  N595AA   1568  DFW      182     1616
```

We see that the flight occurred on March 3rd and departed a little after 2 PM on its way to Dallas/Fort Worth. Lastly, we show how we can visualize the arrival delay of all departing flights from Portland on March 3rd against time of departure.

```
flights %>%
  filter(month == 3, day == 3) %>%
  ggplot(aes(x = dep_time, y = arr_delay)) +
  geom_point()
```

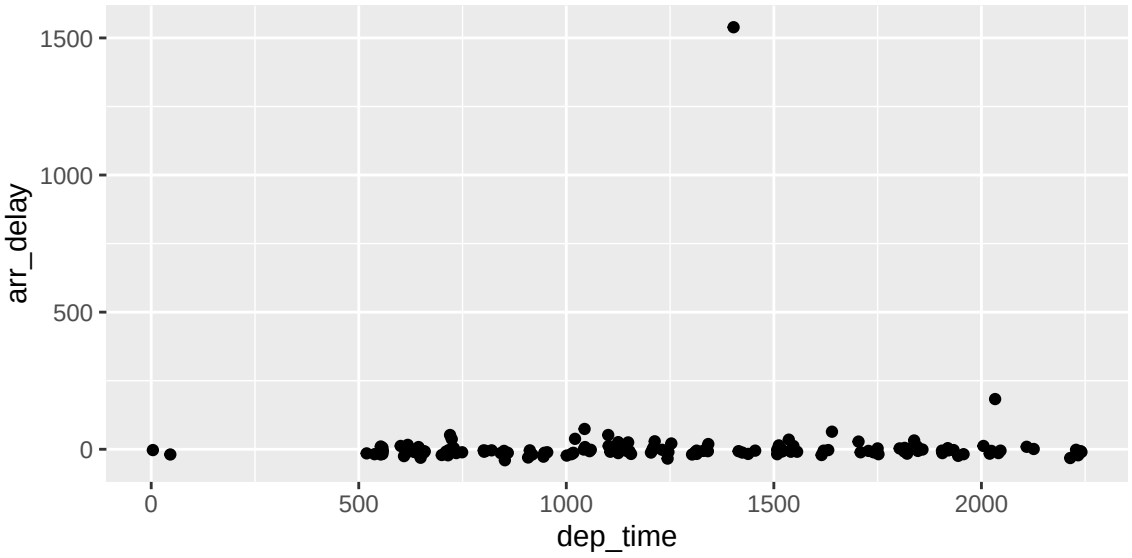

2.7 Additional resources

- *Markdown* Cheatsheet - `https://github.com/adam-p/markdown-here/wiki/Markdown-Cheatshee`

- *R Markdown*
  - Reference Guide - `https://www.rstudio.com/wp-content/uploads/2015/03/rmarkdown-reference.pdf`
  - Cheatsheet - `https://github.com/rstudio/cheatsheets/raw/master/rmarkdown-2.0.pdf`
- *RStudio IDE*
  - Cheatsheet - `https://github.com/rstudio/cheatsheets/raw/master/rstudio-ide.pdf`
  - Official website - `https://rstudio.com/products/rstudio/`
- Introduction to `dplyr` - `https://cran.rstudio.com/web/packages/dplyr/vignettes/dplyr.html`
- `ggplot2`
  - Documentation - `https://ggplot2.tidyverse.org/`
  - Cheatsheet - `https://github.com/rstudio/cheatsheets/raw/master/data-visualization-1.pdf`

2.8 Mathematics and Science

2.9 Math

TEX is the best way to typeset mathematics. Donald Knuth designed TEX when he got frustrated at how long it was taking the typesetters to finish his book, which contained a lot of mathematics. One nice feature of *R Markdown* is its ability to read LaTeX code directly.

If you are doing a thesis that will involve lots of math, you will want to read the following section which has been commented out. If you're not going to use math, skip over or delete this next commented section.

2.10 Chemistry 101: Symbols

Chemical formulas will look best if they are not italicized. Get around math mode's automatic italicizing in LaTeX by using the argument `$\mathrm{formula here}$`, with your formula inside the curly brackets. (Notice the use of the backticks here which enclose text that acts as code.)

So, $Fe_2^{2+}Cr_2O_4$ is written `$\mathrm{Fe_2^{2+}Cr_2O_4}$`.
Exponent or Superscript: O^-
Subscript: CH_4

To stack numbers or letters as in Fe_2^{2+}, the subscript is defined first, and then the superscript is defined.

Bullet: $CuCl \bullet 7H_2O$
Delta: Δ
Reaction Arrows: $\longrightarrow$ or $\xrightarrow{solution}$
Resonance Arrows: $\leftrightarrow$
Reversible Reaction Arrows: $\rightleftharpoons$

2.10.1 Typesetting reactions

You may wish to put your reaction in an equation environment, which means that LaTeX will place the reaction where it fits and will number the equations for you.

$$C_6H_{12}O_6 + 6O_2 \longrightarrow 6CO_2 + 6H_2O \tag{2.1}$$

We can reference this combustion of glucose reaction via Equation (2.1).

2.10.2 Other examples of reactions

$NH_4Cl_{(s)} \rightleftharpoons NH_{3(g)} + HCl_{(g)}$
$MeCH_2Br + Mg \xrightarrow[below]{above} MeCH_2 \bullet Mg \bullet Br$

2.11 Physics

Many of the symbols you will need can be found on the math page `https://web.reed.edu/cis/help/latex/math.html` and the Comprehensive LaTeX Symbol Guide (`https://mirror.utexas.edu/ctan/info/symbols/comprehensive/symbols-letter.pdf`).

2.12 Biology

You will probably find the resources at `https://www.lecb.ncifcrf.gov/~toms/latex.html` helpful, particularly the links to bsts for various journals. You may also be interested in TeXShade for nucleotide typesetting (`https://homepages.uni-tuebingen.de/beitz/txe.html`). Be sure to read the proceeding chapter on graphics and tables.

Chapter 3

Vivianite as a phosphorus source in lake sediments: Importance of increased sulfate reduction on phosphorus mobilization[1]

Abstract

Purpose: Eutrophication of freshwater systems is primarily driven by excessive nutrient inputs, particularly phosphorus (P). While external nutrient control has been emphasized, the prediction and management of internal P loading from sedimentary sources remain complex. This study examines the role of vivianite (Fe(II)$_3$(PO_4_)$_2 \cdot$ 8H_2_O), a P-bearing mineral in anoxic sediments, in contributing to internal P release under sulfidic conditions.

Materials and Methods: A mesocosm experiment was conducted using sediment cores from Lake Arendsee, Germany. The cores were exposed to elevated sulfate concentrations to induce sulfate reduction, simulating anoxic and sulfidic conditions. Both water column chemistry and sediment solid-phase analyses were performed. P release from vivianite-rich sediments was monitored, along with changes in iron (Fe) mineral phases using sequential extraction and X-ray diffraction.

Results and Discussion: Increased sulfate reduction rates significantly mobilized P from vivianite-rich sediments, leading to elevated soluble reactive P levels in the water column. A marked decrease in vivianite content and an increase in sulfide-bound Fe species were observed in the sediments. These findings demonstrate that vivianite in Fe-rich sediments serves as an important internal P source under sulfidic conditions, exacerbating P release.

Conclusions: This study highlights the role of sulfur cycling in internal P loading and suggests that increased sulfate inputs may enhance eutrophication by mobilizing P from buried vivianite. Effective management of eutrophication should consider both external inputs and internal P sources like vivianite.

[1] A modified version of this chapter was published as: van Kuppevelt H, Reitzel K, Hupfer M (2025) Vivianite as a phosphorus source in lake sediments: Importance of increased sulphate reduction on phosphorus mobilisation. J Soils Sediments. https://doi.org/10.1007/s11368-025-03986-z

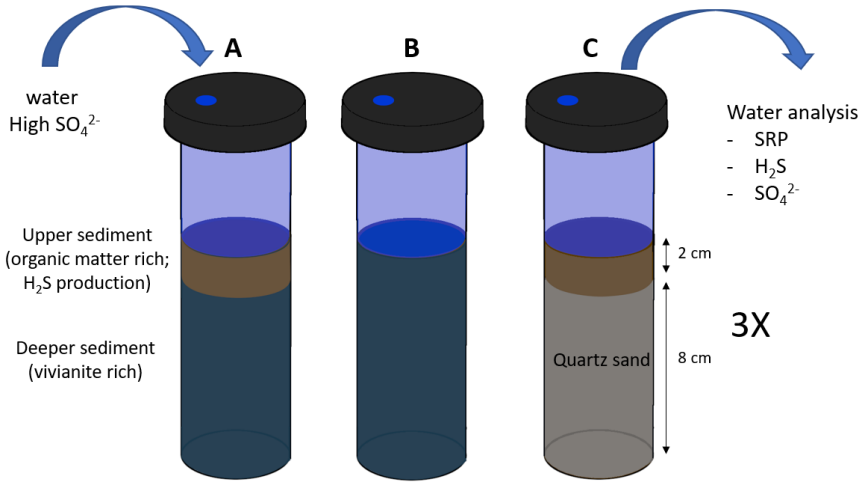

Figure 3.1: Graphic depicting the experimental mesocosm setup: organic matter-rich sediment (OM) was overlain on top of vivianite-rich sediment (Viv.). As control the two types of sediment were also incubated individually, with quartz sand (Qs) below the organic sediment to substitute the volume. At regular intervals, water samples were taken an analysed, and sulphate was replenished.

3.1 Introduction

Eutrophication is a significant environmental issue that affects freshwater systems globally and is driven by an excess of nutrients in water bodies, resulting in excessive algal blooms, oxygen depletion, and diminished water quality (Correll, 1998; Ansari and Gill, 2014). Managing nutrient levels in water is crucial for the restoration of lake ecosystems and the prevention of further degradation. Phosphorus (P) often serves as a limiting factor for primary production and is a focal point for management interventions (Azam and Finneran, 2014; Tammeorg et al., 2024). Despite concentrated efforts on controlling external sources of nutrients such as agricultural runoff and wastewater discharge, water quality targets remain unmet.

For instance, the EU's Water Framework Directive mandates member states to restore lakes within a relatively short time frame [WaterFrameworkDirective2000]. Consequently, contemporary lake management strategies aim to integrate both external and internal measures, with the latter focusing on mitigating the release of P from sediments into the water body (Tammeorg et al., 2024). Managing internal P release can accelerate the effectiveness of reducing external P sources and compensate for high external loads when external measures prove inadequate. A key strategy for internal control involves preventing the release of P from sequestered pools in sediments (burial P). Even after addressing external sources, the internal supply of P can perpetuate eutrophic conditions, especially when the water residence time is high (Søndergaard et al., 2001; Wagner, 2020). However, the processes and sources that drive P release from burial P are not yet fully understood.

The retention of P in sediments occurs through its binding to the solid phase via biological and chemical precipitation (Boers et al., 1998; Parsons et al., 2017; O'Connell et al., 2020).

Burial P pools accumulate in sediment following years of nutrient enrichment. The speciation of sediment P is highly dependent on lake conditions and undergoes significant changes during early diagenesis, where remobilization of labile forms of P occurs, whereas only the stable forms of solid-bound P are buried long-term (Emerson, 1976; Boers et al., 1998). Initially, the sedimentation of P incorporated into organic matter by primary producers is an important influx of P to lake sediments, especially in eutrophic lakes. However, the long-term burial of organic matter-bound P is constrained by remineralization processes in the sediment (Boers et al., 1998). Secondly, P can adsorb to iron (Fe) hydroxides (Gunnars et al., 2002) and bind to organic matter to form organic Fe-P complexes (Schwertmann and Murad, 1988). The precipitation of these ferric Fe-bound P forms (Fe(III)-bound P) can be a major internal sink of P in lakes with naturally high Fe content (Reitzel et al., 2005; Hupfer et al., 2008) or those artificially treated with Fe (Kleeberg et al., 2012; Münch et al., 2024). Under the reducing conditions induced by organic matter decomposition in the sediment, Fe(III) is reduced to Fe(II), leading to the release of bound P and preventing the long-term burial of Fe(III)-bound P. However, P can be sequestered long-term in the form of the Fe(II) mineral vivianite (Fe(II) (PO) · 8H O) (Rothe, 2016), which has been identified as a major form of burial P in eutrophic, high-Fe, and non-sulfidic freshwater systems (O'Connell et al., 2015; Rothe, 2016; Dijkstra et al., 2018; Kubeneck et al., 2021).

The role of sulfur (S) cycling in influencing Fe dynamics and internal P cycling has been recognized as crucial (Kleeberg, 1997; Rozan et al., 2002; Wang et al., 2018; Heinrich et al., 2021), including its impact on vivianite formation (Rothe et al., 2015). Sulfate (SO^{2}) is the dominant form of S in the water column but can be reduced to sulfide (S^{2}) by sulfate-reducing bacteria (SRB) in the sediment during decomposition processes. Sulfide readily binds to Fe, leading to the formation of Fe sulfides such as pyrite (FeS) and Fe monosulfide (FeS). This process effectively immobilizes Fe, removing it from the pool available to form Fe(III)–P or vivianite, thereby affecting the efficiency of P immobilization by Fe in sediments (Heinrich et al., 2020).

An increase in the sulfate reduction rate (SRR) can potentially remobilize the burial pools of Fe–P (Roden and Edmonds, 1997; Katsev et al., 2006). The SRR is influenced by the concentration of sulfate in the sulfate reduction zone, as well as other factors such as temperature (Zhao et al., 2021; Han et al., 2023) and organic matter availability (Chen et al., 2014; Zhao et al., 2019). Several studies have reported a substantial increase in sediment P release following an increase in water sulfate concentrations in both laboratory experiments (Zak et al., 2006; Baldwin and Mitchell, 2012; Chen et al., 2016; Zhou et al., 2022) and in situ studies (Smolders and Roelofs, 1993; Lamers et al., 2002). Over the past century, global freshwater sulfate concentrations have significantly increased because of human activities, remaining well above pre-industrial levels (Kleeberg, 2014; Zak et al., 2021).

The formation of vivianite in lake sediments is a focal point of ongoing research. Evidence of vivianite in older sediment strata underscores the significance of early diagenesis in its formation (Dijkstra et al., 2018; Scholtysik et al., 2022). This phenomenon has also been observed following Fe based treatments implemented for lake restoration (Heinrich et al., 2021). Prior research has identified the availability of Fe(III)–bound P (Heinrich et al., 2020; Kubeneck et al., 2024), redox fluctuations (Parsons et al., 2017), and microbial activity (Cosmidis et al., 2014; Sánchez-Román et al., 2015) as critical environmental factors influencing vivianite formation.

Although vivianite is redox stable and acts as a substantial P sink in anoxic sediments, its long-term stability is not well understood. Vivianite can incorporate significant amounts of P into its structure, contributing notably to the total phosphorus (TP) content in sediments; Rothe (2016) estimated that vivianite-bound P constituted approximately 50% of TP at certain depths in Lake Arendsee (Rothe, 2016). Therefore, if vivianite-bound P pools exist within the sediment, their mobilization could sustain a prolonged release of internal P, exceeding duration estimated from traditional P sources such as Fe(III)–P (Katsev et al., 2006).

Scholars have hypothesized that an increase in sulphide production may lead to sustained P mobilization from buried vivianite by preferentially binding Fe (Roden and Edmonds, 1997; Gächter and Müller, 2003; Katsev et al., 2006). However, this process has not been directly demonstrated in situ, leaving its extent and significance for long-term P release uncertain. In a laboratory setting, Wilfert et al. (2020) demonstrated that pure vivianite released up to 92% of its P when exposed to sulfide (Wilfert et al., 2020). More recently, Kubeneck et al. (2024) demonstrated that this process could also occur under natural pore water conditions by placing synthetic vivianite in mesh bags within the sulfidic sediments of an intertidal flat, resulting in a 30% decrease in vivianite P (Kubeneck et al., 2024).

The present study aimed to further explore the dilapidation of vivianite within freshwater sediments and evaluate its potential contribution to P loading in the water column. This was accomplished by incubating authigenic vivianite in sediments from the sulfidic, dimictic Lake Arendsee in northern Germany, followed by monitoring the dissolution of vivianite and the subsequent release of P over time. Reference figure 2 here 3.2

3.2 Methods

3.2.1 Study Site

Sediment and water samples were collected from Lake Arendsee in northern Germany, located at 52°52'36.12"N, 11°29'12.12"E. Lake Arendsee is a dimictic lake, formed by salt karst processes, and has a relatively long water residence time of 50–60 years. The lake is primarily fed by groundwater and lacks natural drainage (Meinikmann et al., 2015). It reaches a maximum depth of 49.5 meters, an average depth of 29 meters, and covers a surface area of 5.14 km2. Since the 1960s, the lake has undergone significant eutrophication due to urban discharge from the city of Arendsee on the southern shore and drainage from nearby Lake Fauler (Scharf, 1998). P levels in the water column remain elevated due to ongoing groundwater P loading and the accumulation of P from historical inputs, exacerbated by the long water residence time (Hupfer et al., 2019). In addition to high P concentrations (2023 yearly mean of 178 µg L-1; `https://www.igb-berlin.de/der-arendsee`), Lake Arendsee also contains considerable sulfate concentrations (61±7 mg L-1 in January 2023), originating from groundwater influenced by natural geological conditions, including gypsum in the catchment. The organic-rich top sediment layers exhibit significant sulfide production, leading to the formation of Fe sulfide with low total Fe content. In contrast, deeper in the sediment (below approximately 25 cm), the Fe content is much higher, and vivianite is a predominant Fe species (Rothe et al., 2015; Scholtysik et al., 2022).

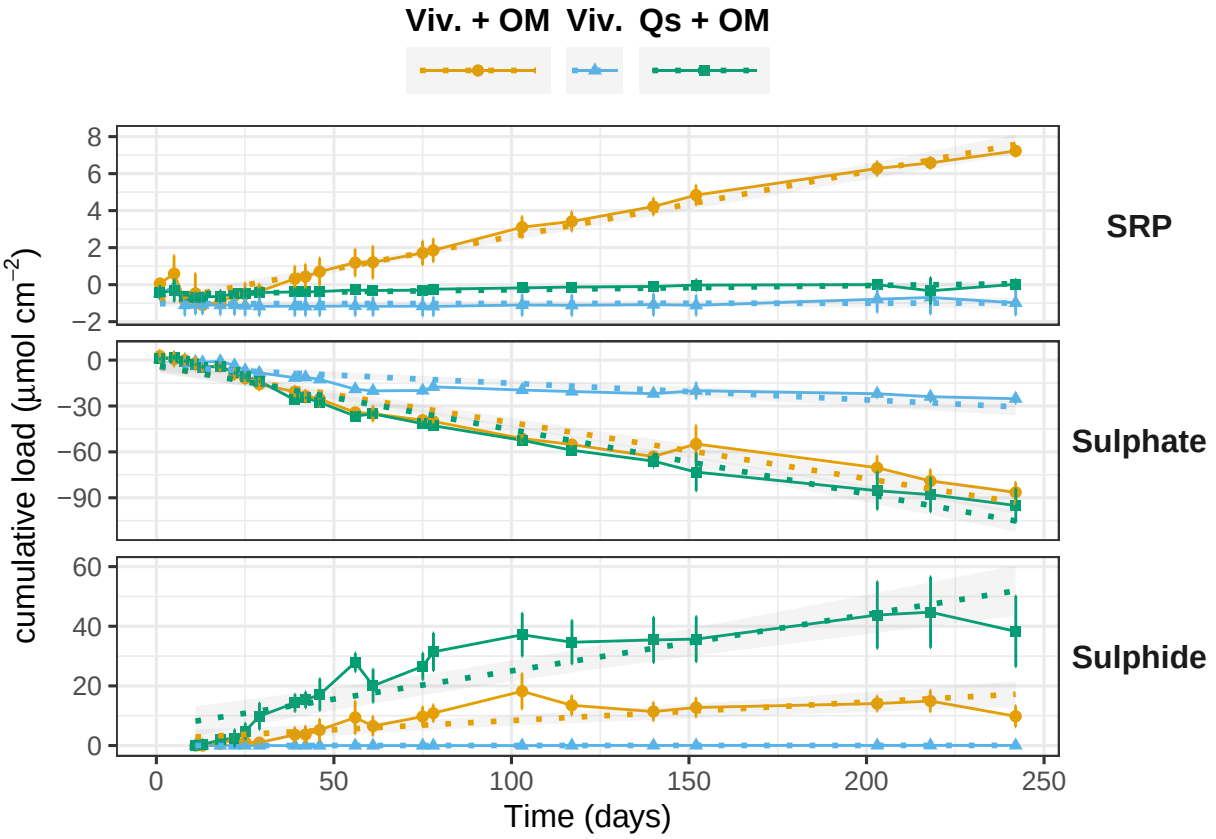

Figure 3.2: Time series of cumulative load of Soluble Reactive Phosphorus (SRP), sulphate, and sulphide to the water column from mesocosm during incubation over a period of approximately 250 days. The change of each species over time was fitted with a linear model, where the slope represents the release rate from the sediment to the water column, which values can be found in Table 2. Viv. + OM: cores with 8 cm of deep (30–35 cm sediment depth), vivianite-rich sediment overlain with 2 cm of sediment rich in organic matter. Viv.: 10 cm of vivianite-rich sediment. Qs + OM: 2 cm of organic matter-rich sediment, on top of 8 cm of quartz sand.

3.2.2 Sample collection

Surface water was collected into a 20 L plastic barrel, from which 10 L were filtered through pressure filtration (0.45 m, cellulose acetate) to remove particulate matter, and then stored in 5 L canisters. Mixed sediment samples were obtained near the lake's deepest points and classified as organic matter-rich upper sediment (0–2 cm) and vivianite-rich deep sediment (30–35 cm). Sediment coring was performed using a UWITEC piston gravity corer with Plexiglas tubes measuring 60 cm in length and 6 cm in diameter. The cores were sectioned on-site, and the selected slices were carefully combined and stored in air-tight Ziplock bags, followed by vacuum sealing to minimize oxygen exposure. The samples were transported immediately to the laboratory and stored at 4 °C for less than a week before the commencement of the experiment. Approximately 2 L of vivianite-rich and 0.5 L of organic matter-rich sediments were collected.

3.2.3 Sulphate reduction experiment

The impact of sulfate reduction on vivianite in natural sediments was investigated by incubating the sediment in controlled mesocosms with added sulfate under anoxic conditions (Fig. 3.1). The incubations were conducted in a climate chamber maintained at 12 °C. Unless otherwise noted, all water used in the experiments was sourced from Lake Arendsee and deoxygenated by bubbling with an N_2/CO_2 mixture for a minimum of 6 h. Within a nitrogen-filled glove bag (Glas-Col 108D X-27-27H, O2 <1%), sealed bags of sediment from Lake Arendsee were opened, transferred to a bucket, and vigorously stirred. For the mesocosm setup, nine Plexiglas tubes—each 30 cm tall and 6 cm in diameter with sliding pistons at the bottom—were prepared in a glove bag for three sets of triplicate treatments. In the first treatment (Fig. 3.1, A), tubes were filled with a combination of vivianite-rich and organic matter-rich sediments (Viv. + OM). In the second treatment (Fig. 3.1, B), only vivianite-rich sediment was used (Viv.). In the third treatment (Fig. 3.1, C), tubes contained only organic matter-rich sediment atop quartz sand, serving as an inert filler to equalise sediment and water column heights across treatments (Qs + OM; Fig. 3.1). Prior to the experiment, tubes designated for treatments Viv. and Viv. + OM were carefully filled with deep vivianite-rich sediment to a depth of 10 cm, ensuring no gas was trapped beneath the sediment. For the Qs + OM treatment, tubes were filled with equivalent volumes of quartz sand. Subsequently, the deoxygenated lake water was poured over the sediment to fill the tubes halfway. The tubes were stagnated overnight to allow the sediment to settle and create a uniform surface for the subsequent layer. The following day, the final sediment layer was added to the mesocosms for treatments Viv. + OM and Qs + OM. For each mesocosm, 60 mL of the upper sediment layer was transferred and allowed to settle at a well-defined sediment-water interface (SWI), after which the height of the water column above the SWI was measured. Thereafter, all tubes were sealed with custom-made airtight caps equipped with stirring magnets and completely filled with anoxic surface water. The sulfate concentration in the overlying water was adjusted to 150 mg L^{-1} (1.6 mmol L^{-1}) by adding approximately 4 mL of a 10.01 g L^{-1} SO_4^{2-} stock solution. Water samples were acquired immediately after setting up the mesocosms to confirm initial sulfate concentrations. The airtight caps ensured the maintenance of anoxic conditions throughout the 242-day incuba-

tion period. Sampling was conducted in a nitrogen atmosphere by flushing the glove bag before opening the caps. Water samples were taken at predetermined intervals, subsampled, and replenished with deoxygenated surface water. Sulfate levels were periodically adjusted to maintain a concentration of 150 mg L^{-1}. After the incubation, the sediment was analyzed to assess the variations in its solid-phase composition.

3.2.4 Sample processing

At the end of the incubation period, the tubes were removed from the glove bag for subsequent processing. The caps were detached, and the final water samples were collected and subsampled before discarding the remaining water, leaving approximately 10 cm above the SWI. Despite air exposure after the removal of the caps and glove bag, the risk of oxygen affecting the sediment prior to slicing was minimal owing to the short duration of exposure compared to the time required for diffusive transport through the water column (hours versus days). The sediment was then sliced to determine the depth profiles of chemical composition and P speciation in the solid phase. To minimize oxygen exposure, sediment processing was conducted immediately and completed within 24 h. Additionally, the exposure was limited by storing the sediments in closed airtight containers, as oxidation can significantly alter P speciation in anoxic sediments (Kraal and Slomp, 2014). The upper 3 cm of the cores were sliced at 0.5 cm intervals, followed by two slices at 1 cm intervals, while deeper layers were sliced at 2 cm intervals down to a depth of 10 cm. The slices were carefully collected and homogenized. Mixed sediment sections were created by pooling equal weights from triplicate slices. This mixed sediment was stored in closed containers at 4 °C overnight, and subsamples were taken the following day for sequential extractions, analysis of dry weight (DW), and loss on ignition (LOI). After subsampling, the mixed sediment was frozen at -20 °C, then freeze dried and ground using an agate mortar and pestle. The dry, powdered sediments were stored in the dark at room temperature and later analysed for elemental and mineralogical composition.

3.2.5 Chemical analysis

Solid phase analysis

The DW and LOI of the sediment samples were determined by weighing approximately 1 g of subsamples, followed by drying at 105 °C for 24 h and combustion at 450 °C for 3 h, respectively. Elemental analysis of the dry sediment was conducted using reverse aqua regia digestion (DIN 38 414-S7, 1983). Approximately 70 mg of dried and ground sediment was digested in 2 mL of 37% HCl and 6 mL of 65% HNO3 in a high-pressure microwave oven (#Prep-A, MLS 169 GmbH). Following dilution, element concentrations were measured by inductively coupled plasma optical emission spectrometry (ICP-OES). To qualitatively assess the mineral composition and identify the presence of vivianite in dry sediment, powder X-ray diffraction (XRD) analyses were conducted. These analyses utilized a Bruker D2 Phaser equipped with a Cobalt X-ray source and an SSD160 detector. Each sample was analysed over a duration of 1 h, covering a range from 10° to 85° 2 , with a step size of 0.014 2 . The device settings included a rotating sample holder, a 1-mm fixed divergence

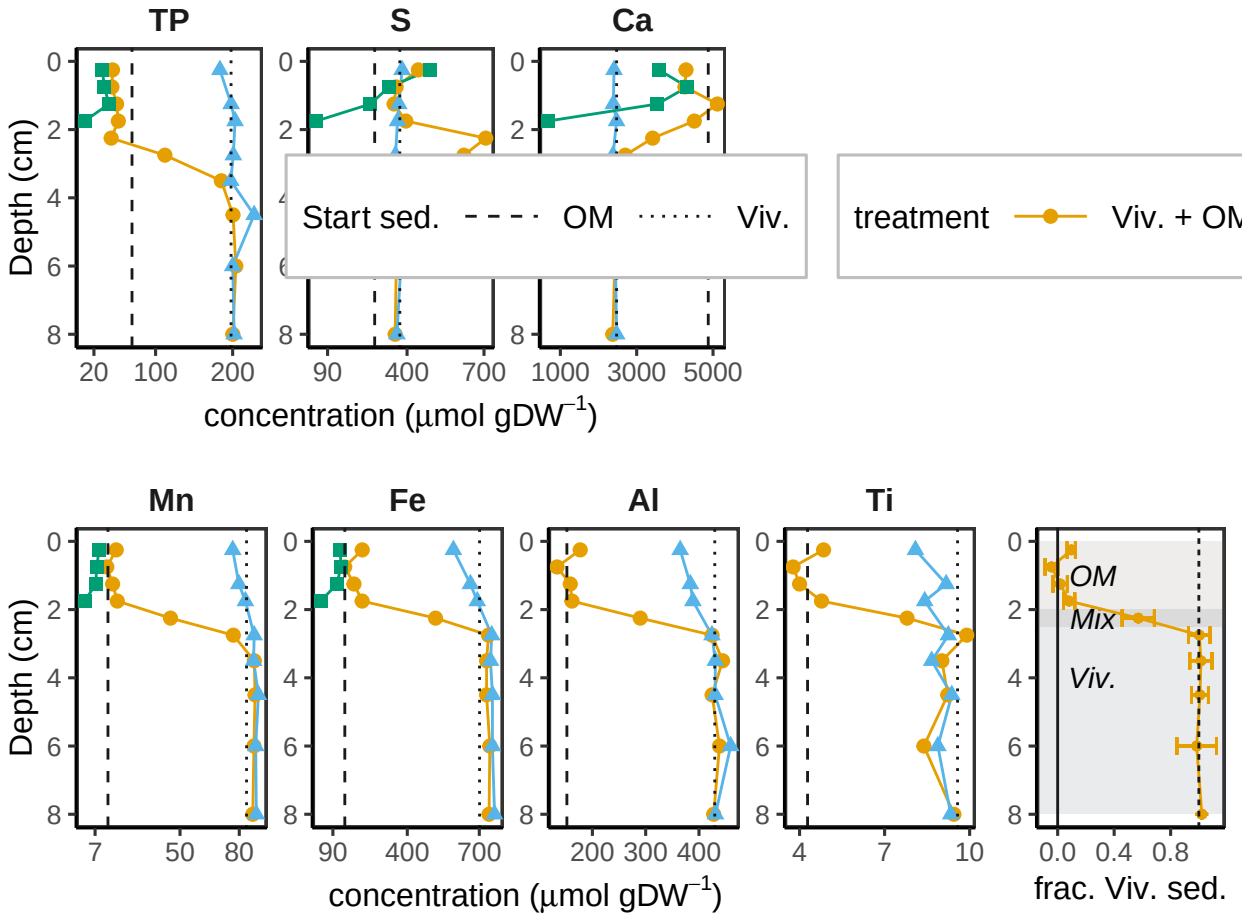

Figure 3.3: Elemental composition profiles of the sediment solid phase of selected elements. The composition of the initial sediment is represented as vertical lines, dotted for deep vivianite-rich sediment and dashed for the upper organic-rich sediment. The last panel shows the proportion of the vivianite-rich sediment in the treatment with both sediment types, where 1 indicates 100% vivianite-rich sediment, while 0 represents 100% OM-rich sediment. Inert elements (aluminium (Al) and Titanium (Ti)), as well Fe and Manganese (Mn) concentrations after incubation were compared to the starting sediment concentrations to determine the sediment type. At the start of the experiment, 2 cm of organic-rich sediment was stacked on top of vivianite-rich sediment. After incubation this was still apparent, while the half centimetre slice between 2.0–2.5 cm depth features a mix of approximately 60%/40% vivianite-rich/OM-rich sediment.

Table 3.1: Sequential extraction steps used in the experiment, based on the protocol of Wang et al. (2021).

Step	Extractant	P fraction	Target P species
1	Deoxygenated MQ H O	H O-P	Labile P, porewater P
2	0.2% 2,2 -bipyridine + 0.1 M KCl	Bipy-P	Vivianite-P, Fe(II)-bound P
3	0.111 M Na S O /0.11 M NaHCO	BD-P	Reducible Fe–P species
4a	0.1 M NaOH	NaOH-SRP	P bound to metals
4b		NaOH-NRP	Biogenic P, difference between TP and SRP
5	0.5 M HCl	HCl-P	Calcium bound P
6	Aqua regia digestion	TP	Total P

slit, 2.5° primary and secondary Soller collimators, a fixed scatter screen at a 3 mm sample distance, and an Fe k-beta filter (2.5). The Bruker DIFFRAC.EVA software was employed for qualitative mineralogical analysis, with mineral identification achieved by comparing results with reference diffractograms from the Crystallography Open Database.

Phosphorus Sequential Extraction

The P and Fe species in the sediment were determined using a sequential extraction protocol, which was originally developed by Psenner et al. (1984) and later modified by Wang et al. (2021) for vivianite extraction (Psenner et al., 1984; Wang et al., 2021). A precisely weighed 0.6 g of wet sediment was placed into 15 mL centrifuge tubes. The extraction process consisted of five steps (Table 3.1). Extracts were filtered, acidified, and analysed for P using the molybdenum blue method (Murphy and Riley, 1962). For the NaOH fraction, extracts were analysed both before and after digestion with $K_2S_2O_8$ to differentiate soluble reactive phosphorus (NaOH-SRP) from nonreactive phosphorus (NaOH-NRP). Specific fractions were designated for Fe analysis (BD-Fe and Bipy-Fe) using Atomic Absorption Spectroscopy (AAS; pinAAcle9001; PerkinElmer, Waltham, MA, USA).

Dissolved elemental analysis

Surface water samples were subdivided into three parts post-filtration (0.22 µm, 0.45 µm cellulose acetate). A 10 mL subsample was preserved with hydrochloric acid for P concentration analysis using the molybdate blue method (Murphy and Riley, 1962). Sulfide concentrations in 2 mL subsamples were fixed with a 2% zinc acetate solution (200 µL) and measured photometrically using the methylene blue method (Cline, 1969). Sulfate concentrations were determined photometrically after filtering through a 0.22 µm cellulose acetate filter, using the BaSO4 colloid method (Tabatabai, 1974). Additionally, the elemental content (Fe, P, S, Mn, Ca, Al, and Ti) of the digested sediment was quantified using inductively coupled plasma optical emission spectroscopy (ICP-OES, iCAP 7000 series, Thermo Scientific).

3.2.6 Data processing and statistical analysis

Data analysis was conducted using R, and the detailed calculations are provided in the Supplementary Material. The release of P, sulfate, and sulfide from the sediment was determined by summing the changes in water column content at each time step, including any added sulfate stock. The variations in sediment composition were assessed by estimating the initial composition based on measurements of starting sediment compositions. This study utilized two types of sediments (Viv. + OM), with the estimated starting composition for each sediment slice derived from the concentrations of unchanged elements (Al, Ti, Fe, and Mn). Concentrations per volume and per surface area, integrated over the measured depths, were calculated from per-dry weight values by estimating the sediment bulk density from dry weight and loss on ignition (LOI) values (Avnimelech et al., 2001). Per-surface area concentrations of dissolved species in the water column were also calculated to compare changes in the solid phase and water column, independent of variations in water column heights. The release rates were determined from concentration time series using the slope of the linear regression. Analysis of Variance (ANOVA) was employed to assess significant differences among the three treatments, followed by Tukey's honestly significant difference (HSD) test to identify the differences in specific treatment. The correlation between sulfate and sulfide concentrations in the water column was analysed using the Pearson correlation coefficient. The significant variations in sediment composition at all depths were tested using a paired t-test, with pairwise comparisons conducted at a 95% family-wise confidence level.

3.3 Results

3.3.1 Sulphate, Sulphide and Phosphorus Dynamics in Overlying Water

All treatments demonstrated a notable reduction in sulphate, resulting in decreased sulphate concentrations compared to the initial and resupplied concentrations of 150 mg L^{-1} (Fig. 3.2). After adjusting for added sulphate stock, the average sulphate reduction rates in treatments with OM sediment were 0.37 and 0.42 µmol cm^{-2} d^{-1}, respectively, both significantly different ($p < 10^{-6}$) from the rate of 0.11 µmol cm^{-2} d^{-1} in the treatment with only vivianite-rich sediments (Table 2). An increase in sulphide levels was observed in the water columns of the Viv. + OM and Qs + OM treatments, with sulphide accumulation correlating with the sulphate decrease (r = -0.73 and r = -0.85, respectively). In the Viv. + OM treatment, sulphide accumulation reached 10 ± 4 µmol cm−2 at the end of the experiment, significantly lower ($p < 0.01$) than in the treatment with Qs + OM (38 ± 12 µmol cm^{-2}). No sulphide accumulation was observed in the treatment with vivianite sediment alone (Fig. 3.2). The release rate of P into the overlying water and the total accumulated SRP in the water column were significantly higher in the Viv + OM treatment, compared to other treatments ($p < 10^{-6}$) (Fig. 2). The initial days of the experiment exhibited fluctuations and a reduction in SRP concentrations as the sediment settled. Following this stabilisation period, SRP levels were lowest in the Viv. treatment sediment, maintaining levels below 10 µmol L^{-1} for most of the experiment. The Qs + OM treatment maintained a slightly higher baseline SRP

concentration at approximately 50 µmol L^{-1}, with minimal SRP release from the sediment (0.0023 µmol cm^{-2} d^{-1}. In contrast, SRP levels in the Viv. + OM treatment continued to increase throughout the experiment, with a release rate of 0.035 µmol cm^{-2} d^{-1} (Table 2).

```
## Warning: Removed 4 rows containing missing values or values outside the scale range
## (`geom_rect()`).
```

3.3.2 Relationship of iron, phosphorus and sulphur in solid sediments

The initial concentrations of total Fe, total phosphorus (TP), and total sulphur (TS) in the sediments before incubation were higher in the Viv-rich deep sediment compared to the OM-rich upper sediment. The treatments did not significantly affect the Fe concentrations in the sediments ($p > 0.5$), with low Fe concentrations observed in the upper 2 cm of treatments containing OM and high Fe concentrations in the Viv. treatment. Similar results were observed for manganese (Mn), aluminium (Al), and titanium (Ti) concentrations, which were used to calculate the proportions of Viv- and OM-type sediments, particularly at the transition between the two sediments in the Viv + OM treatment (Fig. 3.3. Directly below this transition zone, at a depth of approximately 2–3 cm, the largest transformations in composition occurred, particularly in the P and S contents (Figs. 3.3 and 3.4). The TP content in the Viv + OM sediment displayed a significant decrease compared to the initial sediment composition ($p < 0.05$), resulting in an estimated mass loss of 14 µmol cm^{-2} of P after incubation, primarily from the first 3 cm of sediment (Fig. 3.4). In contrast, the TP concentration in the sediment treated with only Viv was not significantly different ($p > 0.1$) from the initial sediment composition (Fig. 3.4.

At the same sediment depth in the Viv + OM treatment where the P content decreased most significantly, the TS content showed a strong increase, peaking at a depth of 2–2.5 cm with a total mass increase of 46 µmol $^{-2}$ S (Table 2). The TS content in the control treatments (Viv and Qs + OM) remained unchanged ($p < 0.05$) compared to that of the respective starting sediments (Fig. 3.4). In addition to significant differences in TP content, the initial sediments exhibited distinct P species, as identified through sequential extractions. Specifically, in the vivianite-rich sediment, the BD-P and NaOH-SRP fractions constituted the largest pools, representing the majority of bound P. Conversely, these fractions, which include Fe-bound P, were the smallest in the OM-rich sediment. The results of the sequential extractions indicated that after incubation, P speciation in the sediments shifted relative to the initial conditions, depending on the treatment and depth. Across all treatments, the uppermost sediment layers were affected; recalcitrant P pools decreased, whereas NaOH-NRP pools slightly increased. In the Viv. + OM treatment, a notable decline in Fe-bound P was observed, with the most significant reductions in the BD-P and NaOH-SRP pools, and the largest relative decrease occurring in NaOH-SRP (Fig. 3.5). XRD analysis of the two initial sediments revealed a characteristic reflection pattern for vivianite in the deeper sediment, absent in the upper sediment (Fig. 6). Post-incubation XRD analysis exhibited a relative reduction in the characteristic peak area in the sediment from the Viv + OM treatment above a depth of 3 cm, with no vivianite detected above a depth of 2.5 cm.

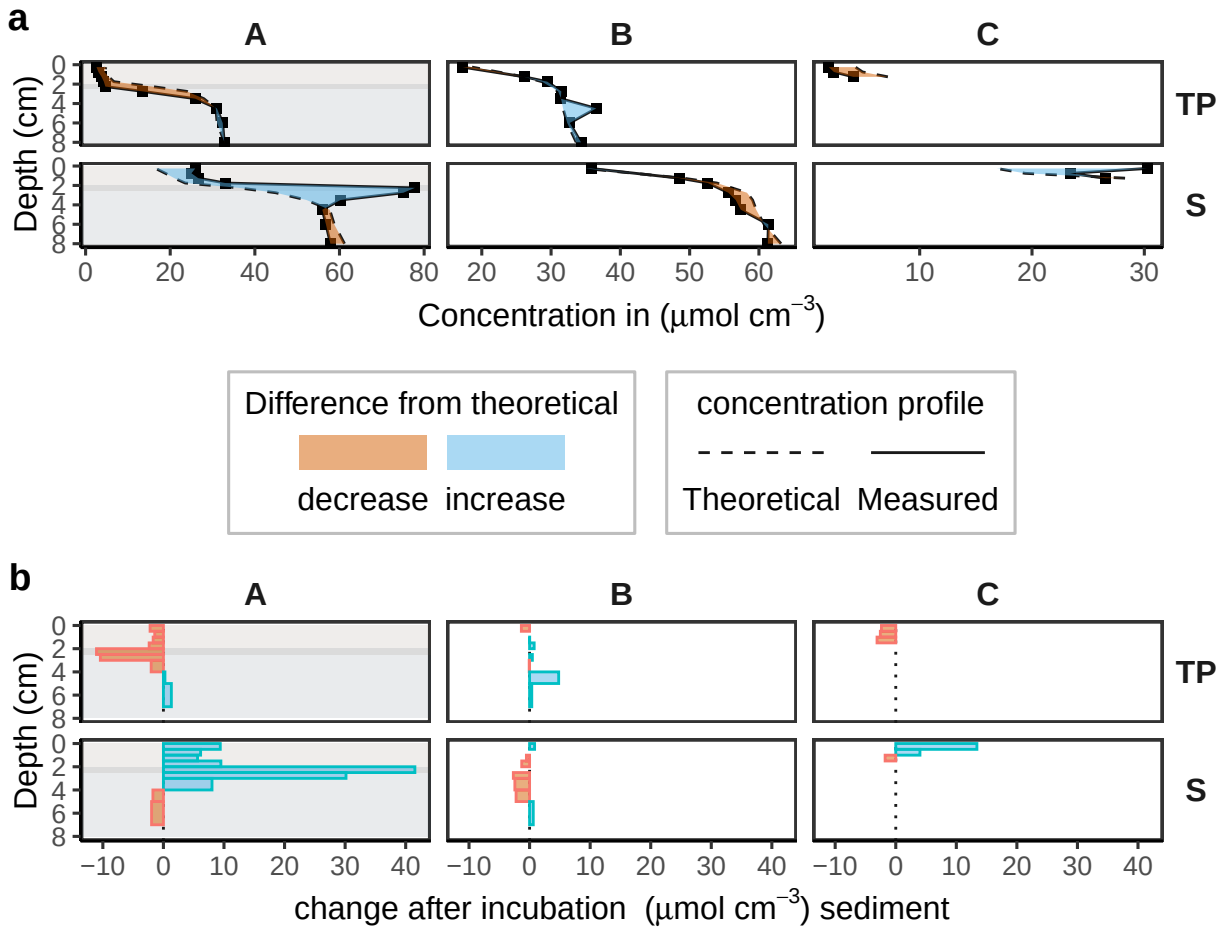

Figure 3.4: Theoretical unchanged concentrations of P and S in the sediment, calculated from the concentrations of the starting sediment, compared with the measured values. The difference is marked as either increase or decrease with respect to the initial composition. (b) The change in sediment P and S content. The surface of the graph represents the total change, and is shown in tables 2 and 3. Total phosphorus (TP) decreased slightly in the upper sediment of treatments with OM, and more significantly in treatment Viv. + OM just below the OM layer between 2 and 3 cm depth. Simultaneously, the S content increased drastically in the same zone.

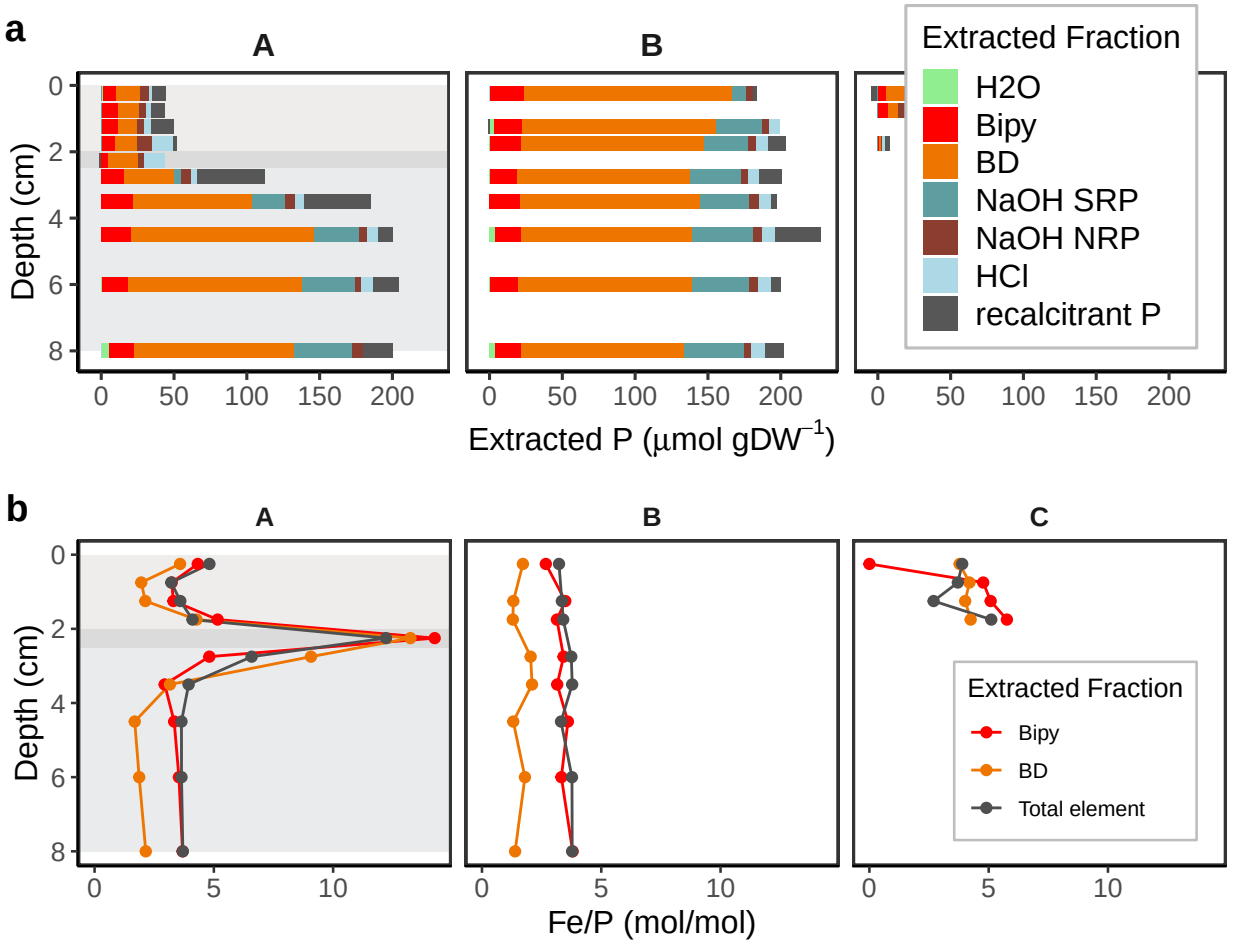

Figure 3.5: Depth profiles of phosphorus (P) fractionation from sequential extractions in three sediment treatment types, depicting the distribution of water-extractable P (H2O-P), 2,2-bipyridine extractable P (Bipy-P), bicarbonate-dithionite extractable P (BD-P), NaOH-extractable soluble reactive P (SRP) and non-reactive P (NRP), HCl extractable P (HCl-P) and total P minus all extracted P (recalcitrant P). (b) Iron over P molar ratio within the sediment total fraction measured by ICP-OES after digestion, and the sequentially extracted Bipyridine and BD fractions. Low Fe/P is indicative for P binding in vivianite and other Fe phases, while high Fe/P suggests low Fe/P binding.

Chapter 4

Paper 3

If we don't want Conclusion to have a chapter number next to it, we can add the `{-}` attribute.

More info

And here's some other random info: the first paragraph after a chapter title or section head *shouldn't be* indented, because indents are to tell the reader that you're starting a new paragraph. Since that's obvious after a chapter or section title, proper typesetting doesn't add an indent there.

Chapter 5

Synthesis

This thesis provides novel insights into the formation, composition, and stability of vivianite in intertidal sediments. This chapter will begin with a summary of the key findings and their potential implications for the role of vivianite in phosphorus (P) cycling in coastal sediments. The discussion will then extend to how the presented findings may apply to various environmental systems and be relevant to other research fields. An examination will follow, discussing how the developed methodology for in-situ studies in this thesis widens our geochemical toolbox and opens various avenues to study in-situ Fe mineral transformation processes. Additionally, this chapter suggests possible directions for future research.

5.1 Summary and discussion

5.1.1 Vivianite stability under sulfidic conditions

The influence of sulphate reduction on phosphorus (P) mobilization i a process found in all aquatic systems, and has been observed in both marine and freshwater systems. Indeed, also in rivers this has been observed (Zak et al., 2006). There are a few key differences why the effect is different in lakes compared to rivers. In lakes, redox stratification often lead to more pronounced sulphate reduction. Secondly, the water residence time is much lower in rivers, and therefore inflow is relatively more important than sediment effects. However, for the same reason an increase of sulfate can be much larger in rivers (Kommana, 2023). As for data on the proportion of phosphorus associated with higher sulphate levels in lakes and rivers, it is important to make a difference between the short and long term. There are many studies that have examined this relationship in the short term in specific systems (e.g. Roden and Edmonds, 1997; Chen et al., 2016; Zhao et al., 2021) . However, as far as I'm aware there is no recent review study. The importance of sulfur on the long term P retention is much more difficult to quantify, although there is some modelling evidence (Katsev et al., 2006) suggesting it may play a major role.

5.1.2 Methodological considerations

Bipyridine extraction. Sediment peeper. Mössbauer, Xanes Synthetic vs natural vivianite.

5.2 Conclusions and outlook

5.2.1 Implications for freshwater management

Diagnostics. Fe treatment. Sulfate management. Dredging.

5.2.2 Relevance to other fields

The RecaP project aims to look in a transdisciplinary fashion at the P challenge, in order to come to a holistic transformation towards sustainable P use. It is therefore crucial to place the implications of this study in a broader context.

further up the P value chain

Stakeholder engagement. Farmer and industry responsibility sulfur mitigation. Reuse of vivianite P from lakes. Lake health as indicator for P recycling success.

Climate change and biodiversity loss

Lakes as biodiversity hotspots and widespread effects of eutrophication

Paleosedimentology and diagenesis

It is interesting to put the relative fluxes of P from antropogenic sources to the geological cycle. Post- depositional alteration of sediment record (Dijkstra et al., 2018) Apatite as main P mineral in geoleogical cycle(Zhao et al., 2024)

5.2.3 Future research

Mössbauer. Find case study where legacy vivianite P is mobilized. Investigate the potential of sulfate management for P control. Develop robust model for predicting Fe treatment efficacy.

Appendix A

The First Appendix

References

A. A. Ansari and S. S. Gill, editors. *Eutrophication: Causes, Consequences and Control*. Springer Netherlands, Dordrecht, 2nd edition edition, 2014. ISBN 978-94-007-7813-9 978-94-007-7814-6. doi: 10.1007/978-94-007-7814-6.

K. Ashley, D. Cordell, and D. Mavinic. A brief history of phosphorus: From the philosopher's stone to nutrient recovery and reuse. *Chemosphere*, 84(6):737–746, Aug. 2011. ISSN 00456535. doi: 10.1016/j.chemosphere.2011.03.001.

Y. Avnimelech, G. Ritvo, L. E. Meijer, and M. Kochba. Water content, organic carbon and dry bulk density in flooded sediments. *Aquacultural Engineering*, 25(1):25–33, Aug. 2001. ISSN 0144-8609. doi: 10.1016/S0144-8609(01)00068-1.

H. M. Azam and K. T. Finneran. Fe (III) reduction-mediated phosphate removal as vivianite (Fe3 (PO4) 2· 8H2O) in septic system wastewater. *Chemosphere*, 97:1–9, 2014.

D. S. Baldwin and A. Mitchell. Impact of sulfate pollution on anaerobic biogeochemical cycles in a wetland sediment. *Water Research*, 46(4):965–974, 2012.

P. C. M. Boers, W. Van Raaphorst, and D. T. Van der Molen. Phosphorus retention in sediments. *Water Science and Technology*, 37(3):31–39, Jan. 1998. ISSN 0273-1223. doi: 10.1016/S0273-1223(98)00053-5.

M. Chen, T.-R. Ye, L. R. Krumholz, and H.-L. Jiang. Temperature and Cyanobacterial Bloom Biomass Influence Phosphorous Cycling in Eutrophic Lake Sediments. *PLOS ONE*, 9(3):e93130, Mar. 2014. ISSN 1932-6203. doi: 10.1371/journal.pone.0093130.

M. Chen, X.-H. Li, Y.-H. He, N. Song, H.-Y. Cai, C. Wang, Y.-T. Li, H.-Y. Chu, L. R. Krumholz, and H.-L. Jiang. Increasing sulfate concentrations result in higher sulfide production and phosphorous mobilization in a shallow eutrophic freshwater lake. *Water Research*, 96:94–104, June 2016. ISSN 00431354. doi: 10.1016/j.watres.2016.03.030.

J. D. Cline. Spectrophotometric Determination of Hydrogen Sulfide in Natural Waters. *Limnology and Oceanography*, 14(3):454–458, 1969. ISSN 1939-5590. doi: 10.4319/lo.1969.14.3.0454.

D. Cordell. *The Story of Phosphorus: Sustainability Implications of Global Phosphorus Scarcity for Food Security*. PhD thesis, 2010.

D. L. Correll. The Role of Phosphorus in the Eutrophication of Receiving Waters: A Review. *Journal of Environmental Quality*, 27(2):261–266, 1998. ISSN 1537-2537. doi: 10.2134/jeq1998.00472425002700020004x.

J. Cosmidis, K. Benzerara, G. Morin, V. Busigny, O. Lebeau, D. Jezequel, V. Noel, G. Dublet, and G. Othmane. Biomineralization of iron-phosphates in the water column of Lake Pavin (Massif Central, France). *Geochimica et Cosmochimica Acta*, 126:78–96, 2014.

N. Dijkstra, M. Hagens, M. Egger, and C. P. Slomp. Post-depositional formation of vivianite-type minerals alters sediment phosphorus records. *Biogeosciences*, 15(3):861–883, 2018.

D. A. Dunnette, D. P. Chynoweth, and K. H. Mancy. The source of hydrogen sulfide in anoxic sediment. *Water Research*, 19(7):875–884, Jan. 1985. ISSN 00431354. doi: 10.1016/0043-1354(85)90146-0.

S. Emerson. Early diagenesis in anaerobic lake sediments: Chemical equilibria in interstitial waters. *Geochimica et Cosmochimica Acta*, 40(8):925–934, 1976.

R. Gächter and B. Müller. Why the phosphorus retention of lakes does not necessarily depend on the oxygen supply to their sediment surface. *Limnology and Oceanography*, 48 (2):929–933, 2003. ISSN 1939-5590. doi: 10.4319/lo.2003.48.2.0929.

A. Gunnars, S. Blomqvist, P. Johansson, and C. Andersson. Formation of Fe (III) oxyhydroxide colloids in freshwater and brackish seawater, with incorporation of phosphate and calcium. *Geochimica et Cosmochimica Acta*, 66(5):745–758, 2002.

T. Han, K. Zhou, J. Chao, X. Xu, T. Zhang, Y. Wang, and M. Kong. Sulfate reduction promotes the release of organic phosphorus and iron-bound phosphorus in black-odor sediments in response to increased temperatures. *Journal of Soils and Sediments*, June 2023. ISSN 1614-7480. doi: 10.1007/s11368-023-03562-3.

L. Heinrich, M. Rothe, B. Braun, and M. Hupfer. Transformation of redox-sensitive to redox-stable iron-bound phosphorus in anoxic lake sediments under laboratory conditions. *Water research*, 189:116609, 2020.

L. Heinrich, J. Dietel, and M. Hupfer. Sulphate reduction determines the long-term effect of iron amendments on phosphorus retention in lake sediments. *Journal of Soils and Sediments*, pages 1–18, 2021.

M. Holmer and P. Storkholm. Sulphate reduction and sulphur cycling in lake sediments: A review. *Freshwater Biology*, 46(4):431–451, 2001.

M. Hupfer, S. Glöss, P. Schmieder, and H.-P. Grossart. Methods for detection and quantification of polyphosphate and polyphosphate accumulating microorganisms in aquatic sediments. *International Review of Hydrobiology*, 93(1):1–30, 2008.

M. Hupfer, A. Kleeberg, and J. Lewandowski. Internal pools and fluxes of phosphorus in dimictic Lake Arendsee, northeastern Germany. *Internal phosphorus loading in lakes: Causes, case studies and management. Plantation, FL, USA: J. Ross Publishing, doi*, 10 (10402381.2020):1756998, 2019.

S. Katsev, I. Tsandev, I. L'Heureux, and D. G. Rancourt. Factors controlling long-term phosphorus efflux from lake sediments: Exploratory reactive-transport modeling. *Chemical Geology*, 234(1-2):127–147, 2006.

A. Kleeberg. Interactions between benthic phosphorus release and sulfur cycling in Lake Scharmützelsee (Germany). *Water, Air, and Soil Pollution*, 99:391–399, 1997.

A. Kleeberg. Eintrag und Wirkung von Sulfat in Oberflächengewässern. In *Handbuch Angewandte Limnologie*, chapter 2.5, pages 1–34. John Wiley & Sons, Ltd, 2014. ISBN 978-3-527-67848-8. doi: 10.1002/9783527678488.hbal2012004.

A. Kleeberg, A. Köhler, and M. Hupfer. How effectively does a single or continuous iron supply affect the phosphorus budget of aerated lakes? *Journal of soils and sediments*, 12 (10):1593–1603, 2012.

A. Kleeberg, C. Herzog, and M. Hupfer. Redox sensitivity of iron in phosphorus binding does not impede lake restoration. *Water research*, 47(3):1491–1502, 2013.

G. Kommana. *Biogeochemical Signatures in Sediments by Iron from Mining Areas: Case Study River Spree (NE Germany)*. PhD thesis, BTU Cottbus-Senftenberg, 2023.

P. Kraal and C. P. Slomp. Rapid and Extensive Alteration of Phosphorus Speciation during Oxic Storage of Wet Sediment Samples. *PLOS ONE*, 9(5):e96859, May 2014. ISSN 1932-6203. doi: 10.1371/journal.pone.0096859.

L. J. Kubeneck, W. K. Lenstra, S. Y. Malkin, D. J. Conley, and C. P. Slomp. Phosphorus burial in vivianite-type minerals in methane-rich coastal sediments. *Marine Chemistry*, 231:103948, 2021.

L. J. Kubeneck, L. Notini, K. A. Rothwell, G. Fantappiè, T. Huthwelker, L. K. ThomasArrigo, and R. Kretzschmar. Transformation of vivianite in intertidal sediments with contrasting sulfide conditions. *Geochimica et Cosmochimica Acta*, Jan. 2024. ISSN 0016-7037. doi: 10.1016/j.gca.2024.01.020.

K. Lalonde, A. Mucci, A. Ouellet, and Y. Gélinas. Preservation of organic matter in sediments promoted by iron. *Nature*, 483(7388):198–200, Mar. 2012. ISSN 1476-4687. doi: 10.1038/nature10855.

L. P. M. Lamers, S.-J. Falla, E. M. Samborska, I. A. R. van Dulken, G. van Hengstum, and J. G. M. Roelofs. Factors controlling the extent of eutrophication and toxicity in sulfate-polluted freshwater wetlands. *Limnology and Oceanography*, 47(2):585–593, 2002. ISSN 1939-5590. doi: 10.4319/lo.2002.47.2.0585.

K. Meinikmann, M. Hupfer, and J. Lewandowski. Phosphorus in groundwater discharge – A potential source for lake eutrophication. *Journal of Hydrology*, 524:214–226, May 2015. ISSN 0022-1694. doi: 10.1016/j.jhydrol.2015.02.031.

M. A. Münch, R. van Kaam, K. As, S. Peiffer, G. ter Heerdt, C. P. Slomp, and T. Behrends. Impact of iron addition on phosphorus dynamics in sediments of a shallow peat lake 10 years after treatment. *Water Research*, 248:120844, Jan. 2024. ISSN 0043-1354. doi: 10.1016/j.watres.2023.120844.

JAMES. Murphy and J. P. Riley. A modified single solution method for the determination of phosphate in natural waters. *Analytica Chimica Acta*, 27:31–36, 1962.

D. W. O'Connell, M. M. Jensen, R. Jakobsen, B. Thamdrup, T. J. Andersen, A. Kovacs, and H. C. B. Hansen. Vivianite formation and its role in phosphorus retention in Lake Ørn, Denmark. *Chemical Geology*, 409:42–53, 2015.

DW. O'Connell, N. Ansems, R. K. Kukkadapu, D. Jaisi, DM. Orihel, BJ. Cade-Menun, Y. Hu, J. Wiklund, RI. Hall, and H. Chessell. Changes in sedimentary phosphorus burial following artificial eutrophication of Lake 227, Experimental Lakes Area, Ontario, Canada. *Journal of Geophysical Research: Biogeosciences*, 125(8):e2020JG005713, 2020.

C. T. Parsons, F. Rezanezhad, D. W. O'Connell, and P. Van Cappellen. Sediment phosphorus speciation and mobility under dynamic redox conditions. *Biogeosciences*, 14(14):3585–3602, July 2017. ISSN 1726-4170. doi: 10.5194/bg-14-3585-2017.

A. Paskin. *Nucleation, Growth and Transformation Phenomena of Vivianite*. PhD thesis, 2024.

R. Psenner, R. Pucsko, and M. Sage. Fractionation of organic and inorganic phosphorus compounds in lake sediments, an attempt to characterize ecologically important Fractions(Die fraktionierung organischer und anorganischer phosphorverbindungen von sedimenten, versuch einer definition okologisch wichtiger fraktionen). *Archiv fur Hydrobiologie*, 1(1), 1984.

K. Reitzel, J. Hansen, F. Ø. Andersen, K. S. Hansen, and H. S. Jensen. Lake Restoration by Dosing Aluminum Relative to Mobile Phosphorus in the Sediment. *Environmental Science & Technology*, 39(11):4134–4140, June 2005. ISSN 0013-936X, 1520-5851. doi: 10.1021/es0485964.

K. Richardson, W. Steffen, W. Lucht, J. Bendtsen, S. E. Cornell, J. F. Donges, M. Drüke, I. Fetzer, G. Bala, W. von Bloh, G. Feulner, S. Fiedler, D. Gerten, T. Gleeson, M. Hofmann, W. Huiskamp, M. Kummu, C. Mohan, D. Nogués-Bravo, S. Petri, M. Porkka, S. Rahmstorf, S. Schaphoff, K. Thonicke, A. Tobian, V. Virkki, L. Wang-Erlandsson, L. Weber, and J. Rockström. Earth beyond six of nine planetary boundaries. *Science Advances*, 9(37):eadh2458, Sept. 2023. doi: 10.1126/sciadv.adh2458.

E. Roden and J. Edmonds. Phosphate Mobilization in Iron-Rich Anaerobic Sediments: Microbial Fe(III) Oxide Reduction Versus Iron-Sulfide Formation. *Archiv fur Hydrobiologie*, 139:347–378, June 1997. doi: 10.1127/archiv-hydrobiol/139/1997/347.

M. Rothe. Exploring vivianite in freshwater sediments. 2016.

M. Rothe, T. Frederichs, M. Eder, A. Kleeberg, and M. Hupfer. Evidence for vivianite formation and its contribution to long-term phosphorus retention in a recent lake sediment: A novel analytical approach. *Biogeosciences*, 11(18):5169–5180, 2014.

M. Rothe, A. Kleeberg, B. Grüneberg, K. Friese, M. Pérez-Mayo, and M. Hupfer. Sedimentary Sulphur:Iron Ratio Indicates Vivianite Occurrence: A Study from Two Contrasting Freshwater Systems. *PLOS ONE*, 10(11):e0143737, Nov. 2015. ISSN 1932-6203. doi: 10.1371/journal.pone.0143737.

T. F. Rozan, M. Taillefert, R. E. Trouwborst, B. T. Glazer, S. Ma, J. Herszage, L. M. Valdes, K. S. Price, and G. W. Luther III. Iron-sulfur-phosphorus cycling in the sediments of a shallow coastal bay: Implications for sediment nutrient release and benthic macroalgal blooms. *Limnology and Oceanography*, 47(5):1346–1354, 2002.

M. Sánchez-Román, F. Puente-Sánchez, and V. Parro. Nucleation of Fe-rich phosphates and carbonates on microbial cells and exopolymeric substances. *Frontiers in microbiology*, 6: 1024, 2015.

B. W. Scharf. Eutrophication history of Lake Arendsee (Germany)1This paper is dedicated to my supervisor Prof. Dr. Harald Sioli in honour of his 85th birthday (25 August 1995).1. *Palaeogeography, Palaeoclimatology, Palaeoecology*, 140(1):85–96, July 1998. ISSN 0031-0182. doi: 10.1016/S0031-0182(98)00033-9.

G. Scholtysik, T. Goldhammer, H. W. Arz, M. Moros, R. Littke, and M. Hupfer. Geochemical focusing and burial of sedimentary iron, manganese, and phosphorus during lake eutrophication. *Limnology and Oceanography*, 67(4):768–783, 2022. ISSN 1939-5590. doi: 10.1002/lno.12019.

U. Schwertmann and E. Murad. The nature of an iron oxide—organic iron association in a peaty environment. *Clay Minerals*, 23(3):291–299, 1988.

A. Smolders and JGM. Roelofs. Sulphate-mediated iron limitation and eutrophication in aquatic ecosystems. *Aquatic Botany*, 46(3-4):247–253, 1993.

M. Søndergaard, P. Jensen, and E. Jeppesen. Retention and Internal Loading of Phosphorus in Shallow, Eutrophic Lakes. *TheScientificWorldJournal*, 1:427–42, Sept. 2001. doi: 10.1100/tsw.2001.72.

M. A. Tabatabai. A Rapid Method for Determination of Sulfate in Water Samples. *Environmental Letters*, 7(3):237–243, Jan. 1974. ISSN 0013-9300. doi: 10.1080/00139307409437403.

O. Tammeorg, I. Chorus, B. Spears, P. Nõges, G. K. Nürnberg, P. Tammeorg, M. Søndergaard, E. Jeppesen, H. Paerl, B. Huser, J. Horppila, T. Jilbert, A. Budzyńska, R. Dondajewska-Pielka, R. Gołdyn, S. Haasler, S. Hellsten, L. H. Härkönen, M. Kiani, A. Kozak, N. Kotamäki, K. Kowalczewska-Madura, S. Newell, L. Nurminen, T. Nõges, K. Reitzel, J. Rosińska, J. Ruuhijärvi, S. Silvonen, C. Skov, T. Važić, A.-M. Ventelä, G. Waajen, and M. Lürling. Sustainable lake restoration: From challenges to solutions. *WIREs Water*, 11(2):e1689, 2024. ISSN 2049-1948. doi: 10.1002/wat2.1689.

K. J. Wagner. Internal phosphorus loading in lakes: Causes, case studies and management. *edited by Alan D.Steinman and Bryan M.Spears: Plantation (FL): J.Ross Publishing, 2020.466 pp.ISBN: 978-1-6042-7822-4*, 2020.

J. Wang, J. Chen, J. Guo, Q. Sun, and H. Yang. Combined Fe/P and Fe/S ratios as a practicable index for estimating the release potential of internal-P in freshwater sediment. *Environmental Science and Pollution Research*, 25(11):10740–10751, 2018.

Q. Wang, T.-H. Kim, K. Reitzel, N. Almind-Jørgensen, and U. G. Nielsen. Quantitative determination of vivianite in sewage sludge by a phosphate extraction protocol validated by PXRD, SEM-EDS, and 31P NMR spectroscopy towards efficient vivianite recovery. *Water Research*, 202:117411, 2021.

P. Wilfert, J. Meerdink, B. Degaga, H. Temmink, L. Korving, G. J. Witkamp, K. Goubitz, and M. C. van Loosdrecht. Sulfide induced phosphate release from iron phosphates and its potential for phosphate recovery. *Water research*, 171:115389, 2020.

D. Zak, A. Kleeberg, and M. Hupfer. Sulphate-mediated phosphorus mobilization in riverine sediments at increasing sulphate concentration, River Spree, NE Germany. *Biogeochemistry*, 80(2):109–119, Oct. 2006. ISSN 0168-2563, 1573-515X. doi: 10.1007/s10533-006-0003-x.

D. Zak, M. Hupfer, A. Cabezas, G. Jurasinski, J. Audet, A. Kleeberg, R. McInnes, S. M. Kristiansen, R. J. Petersen, and H. Liu. Sulphate in freshwater ecosystems: A review of sources, biogeochemical cycles, ecotoxicological effects and bioremediation. *Earth-Science Reviews*, 212:103446, 2021.

M. Zhao, B. J. W. Mills, S. W. Poulton, B. Wan, K.-Q. Xiao, L. Guo, and Z. Guo. Drivers of the global phosphorus cycle over geological time. *Nature Reviews Earth & Environment*, 5(12):873–889, Dec. 2024. ISSN 2662-138X. doi: 10.1038/s43017-024-00603-4.

Y. Zhao, Z. Zhang, G. Wang, X. Li, J. Ma, S. Chen, H. Deng, and O.-H. Annalisa. High sulfide production induced by algae decomposition and its potential stimulation to phosphorus mobility in sediment. *Science of The Total Environment*, 650:163–172, Feb. 2019. ISSN 0048-9697. doi: 10.1016/j.scitotenv.2018.09.010.

Y. Zhao, S. Wu, M. Yu, Z. Zhang, X. Wang, S. Zhang, and G. Wang. Seasonal iron-sulfur interactions and the stimulated phosphorus mobilization in freshwater lake sediments. *Science of The Total Environment*, 768:144336, May 2021. ISSN 0048-9697. doi: 10.1016/j.scitotenv.2020.144336.

C. Zhou, Y. Peng, L. Chen, M. Yu, M. Zhou, R. Xu, L. Zhang, S. Zhang, X. Xu, L. Zhang, and G. Wang. Rapidly increasing sulfate concentration: A hidden promoter of eutrophication in shallow lakes. *Biogeosciences*, 19(17):4351–4360, Sept. 2022. ISSN 1726-4170. doi: 10.5194/bg-19-4351-2022.

List of Figures

List of Tables